Reports

Variations of Rayleigh Wave Phase Velocities across the Pacific Ocean

Abstract. *Rayleigh wave phase velocities on paths crossing the Pacific Ocean show variations which are well correlated with some "average" lithospheric age of the region traversed. The seismic velocities in the upper mantle are highest in the oldest parts of the Pacific and lowest in the youngest parts.*

Many of the physical properties of the oceanic lithosphere are functions of the distance from the ridge crest. Heat flow (*1*), bathymetric depth (*2*), and in some cases gravity (*3*) are among these properties. We have investigated whether the phase velocity of Rayleigh waves also varies with distance from the ridge crest. If this is the case, and we show below that it is, then these variations should be significant diagnostics for determining regional differences in the structure of the upper mantle beneath the oceans (*4*). Furthermore, such variations could provide an explanation for the discrepancy between two recent "standard" oceanic dispersion curves (*5*) obtained by the great circle decomposition method (*6*); the two experiments were made over different parts of the oceans. An alternative explanation is that the discrepancy may be due to refraction at continent-ocean margins (*7*).

We have studied Rayleigh waves along 31 tracks across the Pacific Basin by the single-station method (*8*). In this method the focal mechanism of the earthquake must be known, since there are significant frequency-dependent phase shifts due to the inclination of the focal motions relative to the surface (*9*).

Eleven earthquakes occurring in and around the basin (Table 1) were studied from records of long-period vertical seismometers of the World Wide Standard Seismographic Network located in the basin or on its margin. From the published fault plane solutions for these earthquakes (see Table 1 for references), we have computed the theoretical apparent initial phase of the fundamental mode of the Rayleigh waves by using a program of Schwab and Knopoff (*10*). In the calculation of phase velocities we have assumed that (i) the earthquakes have a step-function time dependence, (ii) displacements at the source can be represented by double-couple force equivalents, (iii) the hypocentral data for the earthquakes are given by the Seismological Bulletin of the National Oceanic and Atmospheric Administration unless a more detailed study is available, and (iv) the structure into which the earthquake radiates is a reasonable approximation to an oceanic structure. With regard to these assumptions, (i) the step function is a reasonable assumption for these shocks, all of which have magnitudes less than 6.5 and thus rupture durations of a few seconds, (ii) the double-couple force equivalent has been demonstrated to be appropriate for a broad range of sources (*11*), (iii) the errors introduced by uncertainties in depth, epicenter, and origin time are small for the magnitudes and distances involved, and (iv) the oceanic structure we have used is a reasonable mean among the structures which we have found to be inverse solutions to our phase velocity results. Three of the epicenters occurred on land, but these were all shallow strike-slip events whose apparent initial phases are independent of structure in the period range of interest.

Digitized seismograms were subjected to harmonic analysis, after selective filtering to suppress effects of interfering signals and noise, and were then corrected for instrumental phase shifts. This procedure yielded an average phase velocity between earthquake epicenter and seismograph for each path. A map of the 31 tracks is shown in Fig. 1, where the epicenters are identified by numbers and the seismic stations by three-letter codes. Four additional paths located in the western marginal seas are also shown in Fig. 1, but data for these paths were not used in this study. In addition, we show the approximate locations of the isochrons of 0, 50, and 100 million years for the Pacific (*2, 12*).

The Rayleigh wave phase velocity curves along seven representative paths are shown in Fig. 2. The lowest phase

Table 1. Earthquakes used in the analysis.

Number	Date	Time	Latitude	Longitude	Depth (km)	Magnitude	Reference
1	7 August 1966	02 13 04.7	50.6°N	171.2°W	39	6.2	(*15*)
2	7 August 1966	17 36 27.3	31.7°N	114.5°W	33	6.5	(*16*)
3	19 January 1967	12 40 09.5	14.8°S	178.7°W	0	6.3	(*17*)
4	9 September 1965	10 02 25.1	6.5°N	84.4°W	0	5.6	(*18*)
5	1 October 1965	08 52 04.4	50.1°N	178.2°E	23	6.3	(*19*)
6	29 July 1965	08 29 21.2	50.9°N	171.4°W	22	6.3	(*15*)
7	20 August 1965	21 21 49.7	22.9°S	176.1°W	79	6.1	(*17*)
8	7 March 1963	05 21 56.6	26.9°S	113.6°W	0	5.8	(*20*)
9	9 April 1968	02 28 59.1	33.2°N	116.1°W	11	6.1	(*21*)
10	6 December 1965	11 34 48.9	18.9°N	107.2°W	0	5.9	(*20*)
11	28 June 1966	04 26 13.4	36.0°N	120.5°W	7	5.5	(*22*)

Scoreboard for Reports: In the past few weeks the editors have received an average of 63 Reports per week and have accepted 11 (17 percent). We plan to accept about 10 reports per week for the next several weeks. In the selection of papers to be published we must deal with several factors: the number of good papers submitted, the number of accepted papers that have not yet been published, the balance of subjects, and length of individual papers.

Authors of Reports published in *Science* find that their results receive good attention from an interdisciplinary audience. Most contributors send us excellent papers that meet high scientific standards. We seek to publish papers on a wide range of subjects, but financial limitations restrict the number of Reports published to about 12 per week. Certain fields are overrepresented. In order to achieve better balance of content, the acceptance rate of items dealing with physical science will be greater than average.

Table 2. Rayleigh wave phase velocities for 50-second periods.

Path	Velocity (km/sec)	Path	Velocity (km/sec)
GUA 1	4.075	RAR 6	4.000
HNR 1	4.072	PEL 7	3.971
AFI 2	3.986	SOM 7	3.973
BAG 2	4.014	KIP 8	3.930
DAV 2	4.030	AFI 9	4.000
GUA 2	4.064	BAG 9	4.011
HNR 2	4.022	DAV 9	4.024
PMG 2	4.019	ANT 10	3.857
RAB 2	4.019	ARE 10	3.808
RIV 2	3.965	GIE 10	3.746
BHP 3	3.963	PEL 10	3.860
LPB 3	3.941	RIV 10	3.979
GUA 4	4.018	TAU 10	3.978
LON 5	3.943	WEL 10	3.972
AFI 6	4.022	SBA 11	3.909

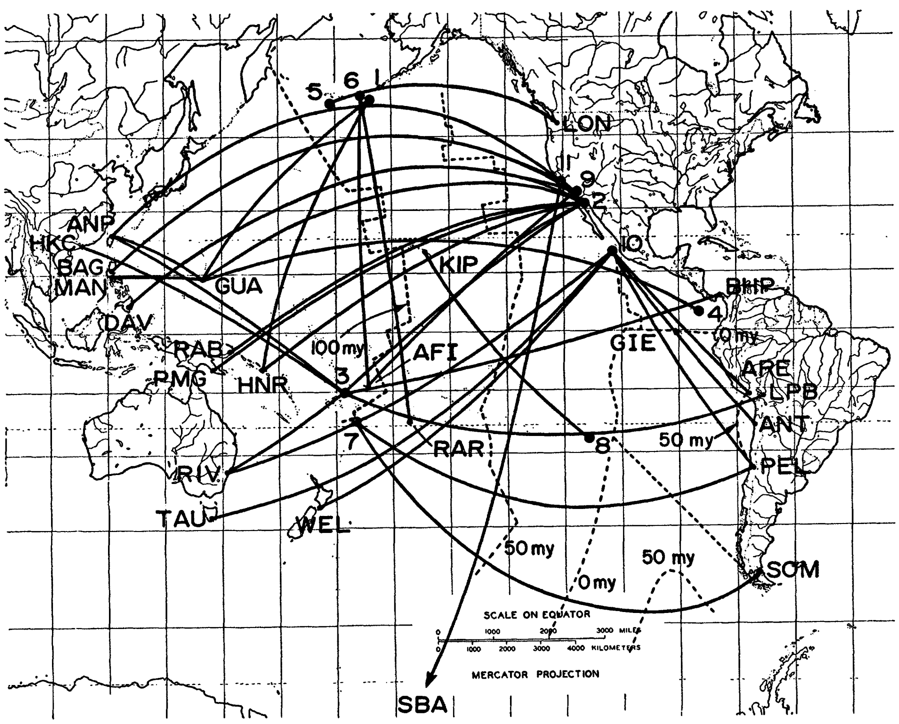

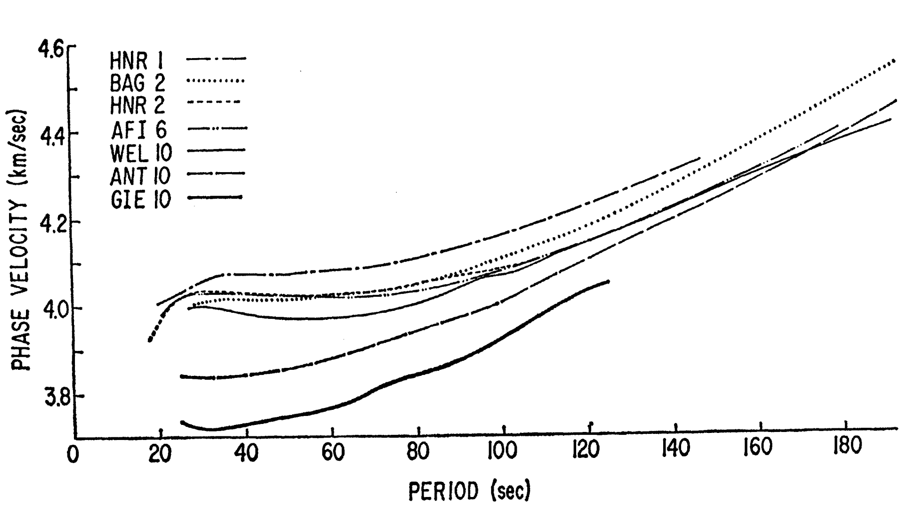

Fig. 1 (top). Great circle paths traversing the Pacific Ocean used in the analysis. The numbers identify the earthquakes (see Table 1) and the three-letter codes the seismic stations. Isochrons of 0, 50, and 100 million years (*my*) are shown. Fig. 2 (bottom). Rayleigh wave phase velocities for seven representative paths across the Pacific Ocean.

velocities on any of the 31 paths were found for the path GIE 10, which follows the crest of the East Pacific Rise. The highest velocities were found on paths HNR 1 and GUA 1; the result for HNR 1 is shown in Fig. 2. In general, phase velocities were similar along paths lying close to one another; for example, the phase velocities on paths PMG 2 and RAB 2 differed by less than 0.007 km/sec over the period range 30 to 140 seconds; the phase velocities on AFI 2 and AFI 9 differed by less than 0.016 km/sec over the same period range. Since these differences are much less than the differences observed for paths remote from one another, we interpret the latter differences as being due to regional variations in the structure of the upper mantle.

We find that the Rayleigh wave phase velocities increase systematically with some average lithospheric age for the path. We leave unanswered the question of the nature of the averaging of the ages involved in the correlation, since a detailed inversion is presented in the accompanying report (*13*). The phase velocities on path GIE 10, which follows the crest of the ridge, are significantly lower than those on path ANT 10, which is the extension of GIE 10 across the Nazca plate; the age on ANT 10 is greater than that on GIE 10.

In the central Pacific, the phase velocities on paths WEL 10, HNR 2, and BAG 2 systematically increase with the age of the region traversed, with the largest values for the northernmost path. The phase velocities of the central Pacific group of paths are all higher than those of the southeastern Pacific group, and the ages are similarly greater.

The highest phase velocities were found for paths lying in the oldest regions. The phase velocities for GUA 1 and HNR 1 are slightly higher than those for the younger path AFI 6, which, in turn, are higher than those for the still younger path RAR 6.

The correlation between phase velocity and age is found for all 31 examples without notable exceptions. Phase velocities at a representative period of 50 seconds are listed in Table 2 for 30 of the paths (*14*).

We believe the differences among the phase velocities are significant indicators of changes in upper mantle structure beneath the Pacific Ocean. The heterogeneity in phase velocities may also serve to explain differences in phase velocity measurements obtained from globe-circling paths. The systematic changes in phase velocities, amounting to about 10 percent between the extreme cases, cannot be explained by noise on the records or some random property of lithospheric structure. The results show that there is a local change in Rayleigh wave phase velocity which indicates that there is a local change in upper mantle *S*-wave velocity. These changes in velocity are correlated with lithospheric age.

EDGAR G. KAUSEL*
ALAN R. LEEDS†
LEON KNOPOFF

Institute of Geophysics and Planetary Physics, University of California, Los Angeles 90024

References and Notes

1. W. H. K. Lee and S. Uyeda, in *Terrestrial Heat Flow*, W. H. K. Lee, Ed. (American Geophysical Union, Washington, D.C., 1965), p. 87.
2. J. G. Sclater and J. Francheteau, *Geophys. J. R. Astron. Soc.* **20**, 509 (1970).
3. W. M. Kaula, *Science* **169**, 982 (1970); in *The Nature of the Solid Earth*, E. C. Robertson, Ed. (McGraw-Hill, New York, 1972), p. 385; *J. Geophys. Res.* **74**, 4807 (1969); K. Lambeck, *Geophys. J. R. Astron. Soc.* **30**, 37 (1972).
4. J. Dorman, M. Ewing, J. Oliver, *Bull. Seismol. Soc. Am.* **50**, 87 (19(L. Knopoff, *Tectonophysics* **13**, 497 (1972).
5. H. Kanamori, *Phys. Earth Planet. Interiors* **2**, 259 (1970); A. Dziewonski, *Geophys. J. R. Astron. Soc.* **22**, 289 (1971).
6. M. N. Toksöz and D. L. Anderson, *J. Geophys. Res.* **71**, 1649 (1966).
7. R. Madariaga and K. Aki, *ibid.* **77**, 4421 (1972).
8. J. N. Brune, J. E Nafe, J. Oliver, *ibid.* **65**, 287 (1960).
9. L. Knopoff and F. A. Schwab, *ibid.* **73**, 755 (1968).
10. F. A. Schwab and L. Knopoff, in *Methods in Computational Physics*, B. A. Bolt, Ed. (Academic Press, New York, 1972), vol. 11, p. 87.
11. R. Burridge and L. Knopoff, *Bull. Seismol. Soc. Am.* **54**, 1875 (1964).
12. E. Herron, in *Antarctic Oceanology I*, vol. 15 in *Antarctic Research Series*, J. L. Reid, Ed. (American Geophysical Union, Washington, D.C., 1971), p. 229; R. C. Larson and C. G. Chase, *Geol. Soc. Am. Bull.* **83**, 3627 (1972).
13. A. R. Leeds, L. Knopoff, E. G. Kausel, *Science* **186**, 141 (1974).
14. Phase velocities for path ANP 9 were measured over the period range 100 to 190 seconds.

W. Stauder, *J. Geophys. Res.* **73**, 7693 (1968).

16. A. R. Leeds, thesis, University of California, Los Angeles (1973).
17. B. Isacks, L. R. Sykes, J. Oliver, *Geol. Soc. Am. Bull.* **80**, 1443 (1969).

P. Molnar and L. R. Sykes, *ibid.*, p. 1639.

W. Stauder, *J. Geophys. Res.* **73**, 3847 (1968).

L. R. Sykes, *ibid.* **72**, 2131 (1967).

21. C. R. Allen and J. M. Nordquist, *U.S. Geol. Surv. Prof. Pap. 787* (1972), p. 16.
22. T. V. McEvilly, W. M. Bakun, K. B. Casaday, *Bull. Seismol. Soc. Am.* **57**, 1221 (1967).

23. Supported by the Earth Sciences Section, National Science Foundation (grants GA-37119X and GA-18673). Publication No. 1267, Institute of Geophysics and Planetary Physics, University of California, Los Angeles.

* Present address: Department of Geophysics, University of Chile, Santiago.

† Present address: Lamont-Doherty Geological Observatory, Columbia University, Palisades, New York 10964.

20 June 1974

Variations of Upper Mantle Structure under the Pacific Ocean

Abstract. *The inversion of Rayleigh wave dispersion data for the Pacific Ocean shows that lithospheric thickness increases systematically with age. The lid to the low-velocity channel is very thin or absent near the ridge crest; the low-velocity channel may be absent in the oldest parts of the ocean.*

Observations of the dispersion of Rayleigh waves indicate that there is significant heterogeneity in the structure of the upper mantle beneath the Pacific Ocean (*1*). The heterogeneity is sufficiently well correlated with lithospheric age for this to form the most appropriate basis for inversion of the observations at this time. In a sense, the use of lithospheric ages provides one coordinate of a system for the Pacific Ocean. In the absence of any theory for the variation of dispersion in the Pacific, we see no particular reason to use surface harmonic or polynomial expansions of observations (*2*) or indeed to use functions of any coordinate system obtained from geographical considerations as a basis for inversion.

The geophysical inverse problem is a search for a certain class of models; specified mathematical operations on these models yield a set of values which fit the observations within a specified accuracy (*3*). Two methods of analysis can be considered for the inverse problem. In the most popular procedure, the observations of dispersion on paths crossing a large area are decomposed into regional dispersion relations, which can then be inverted to give local structure (*2, 4, 5*). However, this procedure may mask the fact that models constructed for one region depend interactively on models constructed for other regions. The construction of regionalized dispersion curves may generate a data base with apparently more degrees of freedom than are present in the original data set. In the case of a system with only 5 degrees of freedom in the original dispersion data, one would not be able to adjust the 16 parameters of lid and channel thickness and velocity in each of four geographic regions independently; however, the construction of regionalized dispersion curves from the original data set might give the illusion that 4 degrees of freedom were present in each of the dispersion curves.

Table 1. Regionalized lithospheric ages and lengths of paths.

Region	Average age (million years)	Total path length (km)
1	150	26309
2	120	18716
3	100	60716
4	70	34872
5	50	44884
6	30	39455
7	15	19295
8	5	23278

In the method of analysis we used, the dispersion measurements are inverted directly into regional upper mantle structures; the interplay of regional structural parameters is adjusted so that the sums of the phase delays across each region match the observations in an appropriate manner. The regional dispersion relations can then be derived from the regional structure.

We used a subdivision of the Pacific Basin into eight zones, each having a different value of lithospheric age (*6*) (Table 1), plus a ninth zone which represents the marginal seas behind island arcs. The first eight regions represent a subdivision of the tectonic history of the upper mantle of the Pacific from ridge to trench. The input data were 182 Rayleigh wave phase velocities, sampled at selected periods from 30 seconds to the longest periods available, for 31 paths; the longest period used was 190 seconds. The total length of the paths traversing each age region is given in Table 1. Since a significant fraction of the total path length is spent in region 9, independent measurements were made of phase velocities for four paths wholly in the marginal seas and were used to correct the phase velocities for the 31 paths in the eight regions (*7*). Corrections to the phase velocities were $\lesssim 0.02$ km/sec. Each phase velocity measurement was weighted in the inversion according to the total path length and period, the longer path lengths and shorter periods having the greater weighting factors.

We report results for five related numerical inversion experiments, which differ in the nature of the constraints used in parameterizing the models. Certain features of the parameterization were preserved in all five experiments. The crust and upper mantle were divided into a small number of layers: the water layer, the crust including sediments, the lid to the low-velocity channel, the low-velocity channel, and the subchannel regions. Below the subchannel, and beginning at a depth of ~ 450 km, there is a standard platform (*8*). The lithosphere consists of the crust and the lid, and the asthenosphere is taken to be the low-velocity channel. In each region the thickness of crust and depth of water were chosen to match best local estimates. The *P*-wave velocities (V_P) and densities for the layers were not used as variables, and the *S*-wave velocities (V_S) in the crust and platform were fixed. The *S*-wave velocities in the lid, channel, and subchannel and the depths to the interfaces between these layers